



SPE 77551

## Engineering Calculations of Gas Condensate Well Productivity

Robert Mott, SPE, ECL Technology Limited

Copyright 2002, Society of Petroleum Engineers Inc.

This paper was prepared for presentation at the SPE Annual Technical Conference and Exhibition held in San Antonio, Texas, 29 September–2 October 2002.

This paper was selected for presentation by an SPE Program Committee following review of information contained in an abstract submitted by the author(s). Contents of the paper, as presented, have not been reviewed by the Society of Petroleum Engineers and are subject to correction by the author(s). The material, as presented, does not necessarily reflect any position of the Society of Petroleum Engineers, its officers, or members. Papers presented at SPE meetings are subject to publication review by Editorial Committees of the Society of Petroleum Engineers. Electronic reproduction, distribution, or storage of any part of this paper for commercial purposes without the written consent of the Society of Petroleum Engineers is prohibited. Permission to reproduce in print is restricted to an abstract of not more than 300 words; illustrations may not be copied. The abstract must contain conspicuous acknowledgment of where and by whom the paper was presented. Write Librarian, SPE, P.O. Box 833836, Richardson, TX 75083-3836, U.S.A., fax 01-972-952-9435.

### Abstract

The productivity of many gas condensate wells is reduced by the formation of a condensate bank in the near-well region. Forecasting of gas condensate well productivity usually requires fine-grid numerical simulation to model the formation of the condensate bank, and to account for high-velocity phenomena such as non-Darcy flow and changes in relative permeability at large capillary numbers.

This paper presents a new technique for forecasting performance of gas condensate wells, using simpler techniques, which can be used in a spreadsheet. The calculation uses a material balance model for reservoir depletion and a two-phase pseudopressure integral for well inflow performance. The pseudopressure integral technique has been extended to include high-velocity effects and also to allow for the change in produced fluid composition due to the formation of the condensate bank.

The new technique has been tested by comparison with the results of fine-grid compositional simulation, and the results are in good agreement for a wide range of cases covering vertical, horizontal and hydraulically fractured wells.

The spreadsheet model provides a useful tool for rapid forecasts of condensate well performance, for examining the effects of condensate blockage in different well types or for studying sensitivities. It is also valuable where simple models of condensate reservoir performance are required for use in integrated studies involving issues such as surface facilities, drilling schedules and gas sales contracts.

### Introduction

Well productivity is an important issue in the development of most low and medium permeability gas condensate reservoirs. However, accurate forecasts of productivity can be difficult

because of the need to understand and account for the complex processes that occur in the near-well region.

When the well pressure falls below the dew point, a region of high liquid saturation builds up around the well, impairing the flow of gas and reducing productivity. It is essential to take account of this 'condensate blockage' effect when calculating well productivity.

Most of the drawdown to a condensate well occurs close to the wellbore, where gas velocities may be very high, and the relationship between flow rate and pressure drop may be complicated by two additional phenomena.

1. The increase in mobility at high capillary number<sup>1,2,3,4</sup>, sometimes referred to as 'positive coupling' or 'viscous stripping'.
2. Inertial or non-Darcy flow.

In most gas condensate wells the net effect of the two high-velocity phenomena is to improve productivity, reducing the impairment due to condensate blockage, and it is important to include these high-velocity effects when simulating gas condensate well performance. The importance of high-velocity effects has been demonstrated by history matching results for a number of wells, where it was only possible to obtain a satisfactory match when high-velocity effects were included in the simulation model<sup>5,6</sup>.

### Well Productivity Calculations

The most accurate way of calculating gas condensate well productivity is by fine-grid numerical simulation, either in single-well models with a fine grid near to the well, or in full field models using local grid refinement. A fine-grid model will allow for high-velocity effects to be modeled, and most commercial simulators now include options to account for inertial flow and the increase in mobility at high capillary number.

While numerical simulation is suitable for detailed forecasting of reservoir behaviour, there are many applications where this level of modeling is not justified, and simpler engineering calculations are more appropriate.

Simpler calculations are particularly useful to provide rapid forecasts of well deliverability, for sensitivity studies to assess the impact of parameters such as relative permeability or PVT properties, or to estimate the benefits of fractured or horizontal wells. They may also be more appropriate where accurate data on reservoir, fluid or rock properties are not available.

Another application of a simple reservoir model is as part of an integrated study involving issues such as pipelines, surface facilities, drilling schedules and gas sales contracts. This type of integrated model can also be used with Decision Risk Management techniques to optimise development strategies, while taking account of uncertainties in reservoir data or financial parameters<sup>7</sup>.

**Material Balance Model.** A simple approach to forecasting gas condensate reservoir performance is to use a material balance model combined with a well inflow-performance-relationship (IPR). The material balance model can be linked to an analytic aquifer model if necessary.

Fluid PVT properties are calculated from an extended black oil model, where properties such as oil-gas ratio and formation volume factor are tabulated against pressure. Simulation studies have shown no significant difference between extended black oil and compositional simulator results for gas condensate reservoirs under depletion<sup>8,9</sup>, so that a black oil model is perfectly adequate for the engineering calculations in this work.

The well IPR is based on the pseudopressure integral method, which can take account of condensate blockage, including the impact of high-velocity effects. The application of the pseudopressure integral is discussed in detail in the following section.

The well IPR is used to calculate the maximum gas production rate from the well at a particular value of the average reservoir pressure. This rate is then adjusted to allow for any well or facilities limits, resulting in a table of gas rate versus average reservoir pressure. The pressure intervals in this table are the same as in the input table of PVT properties, typically at intervals of 200 to 500 psi. From this table, production profiles can be calculated giving oil and gas production rates as a function of time.

### Well Inflow Calculation

**Pseudopressure Integral.** The well gas production rate is given by

$$Q_g = \gamma [m(P_{res}) - m(P_w)] \quad (1)$$

where  $\gamma$  is the productivity index which depends on the well and reservoir geometry and is discussed in Appendix A, and  $m(P)$  is the 2-phase pseudopressure, defined by<sup>10</sup>

$$m(P) = \int_{P_{ref}}^P \left[ \frac{k_{rg}}{\mu_g B_g} + \frac{k_{ro} R_s}{\mu_o B_o} \right] dP \quad (2)$$

In order to evaluate the pseudopressure integral, the region around the well is divided into three regions as proposed by Fevang and Whitson<sup>10</sup>

1. An inner region where both gas and oil (condensate) phases are flowing.
2. A region of condensate build-up where only the gas phase is flowing. An oil phase is present but is immobile.
3. A region where only the gas phase is present.

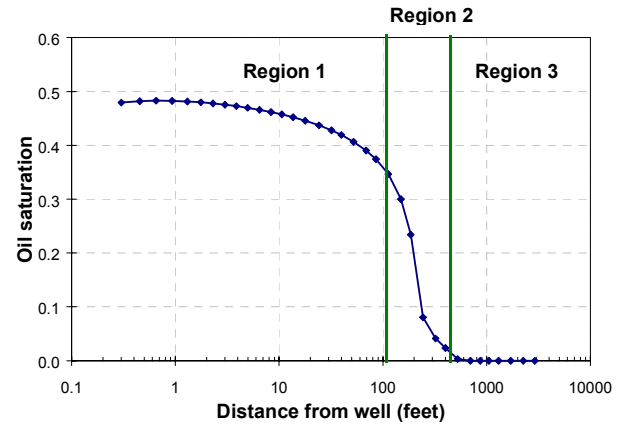


**Fig. 1. Oil phase saturation around a vertical, unfractured well. Note log scale for distance from well.**

Fig 1 shows the oil saturation profile for a vertical, unfractured well, with the three regions indicated. Note the logarithmic scale for the distance from the well. In this example, the average reservoir pressure is above the dew point pressure, and the well bottom hole pressure is below the dew point, so that all three regions are present.

At a given time in the reservoir's production history, one, two or three of the regions may exist. However, when the well bottom hole pressure has fallen below the dew point pressure and condensate blockage has become a problem, most of the pressure drawdown will occur in Region 1, so that accurate evaluation of Region 1 is crucial to the calculation of the pseudopressure integral.

Fevang and Whitson<sup>10</sup> pointed out that the flowing composition is constant in Region 1. This is illustrated in Fig. 2, which shows the flowing oil-gas ratio (OGR), made up of the combined flow in both oil and gas phases. (The flowing OGR refers to the ratio of stock tank oil and dry gas in the black oil PVT model.)

If the flowing OGR  $r_{vF}$  is known, the ratio  $k_{rg}/k_{ro}$  in Region 1 can be calculated as a function of pressure from the equation<sup>10</sup>

$$\frac{k_{rg}}{k_{ro}} = \frac{1 - r_{vF} R_s}{r_{vF} - r_v} \frac{\mu_g B_g}{\mu_o B_o} \quad (3)$$

If the ratio of  $k_{rg}/k_{ro}$  is known, the values of  $k_{rg}$  and  $k_{ro}$  can be calculated from the relative permeability curves, and the pseudopressure integral calculated.

**Importance of the flowing OGR in Region 1.** A key part of evaluating the pseudopressure integral is the estimation of the flowing OGR at the well and in Region 1,  $r_{vF}$ . The simplest method is to assume that  $r_{vF}$  is equal to the flowing OGR in the deep reservoir, far from the well. If the liquid phase is immobile far from the well, the flowing OGR in the deep reservoir is equal to saturated gas OGR at the average reservoir pressure. This assumption for  $r_{vF}$  is termed the

‘CVDMB method’ in Ref. 10. However, in practice this approach will almost always overestimate  $r_{vF}$ .

Fig. 2 illustrates how the CVDMB method can overestimate the flowing OGR. The saturated gas OGR at the average reservoir pressure is 165 stb/MMscf, whereas the flowing OGR in Region 1 is 151 stb/MMscf. The change in OGR is due to the loss of oil in Region 2 as the condensate bank builds up around the well.

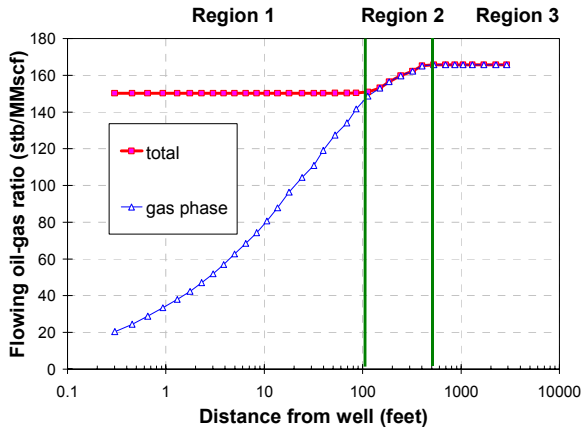


Fig. 2. Flowing oil-gas ratio to a vertical, unfractured well.

A good estimate of  $r_{vF}$  is important if the pseudopressure integral is to give an accurate model of the well inflow. In the example given here, changing  $r_{vF}$  from 151 stb/MMscf to 165 stb/MMscf reduces the value of the pseudopressure integral by about 20%, so that the CVDMB method of estimating  $r_{vF}$  would underestimate the well productivity significantly.

When the pseudopressure integral is used within a coarse grid reservoir simulation model, the simulator will give a reasonable estimate of  $r_{vF}$  provided that the well grid block size is not too large<sup>10,11</sup>. In a material balance model, a new method must be devised to estimate the flowing OGR in Region 1.

**Calculating the flowing OGR in Region 1.** The new method for calculating  $r_{vF}$  is based on estimating the volume of Region 1, as  $r_{vF}$  is equal to the OGR of saturated gas at  $P_1$ , the pressure at the outer edge of Region 1. Fig 3 is based on the same data as Figs. 1 and 2, and shows the flow rate of stock tank oil as a function of distance from the well. This shows that the oil flow rate reaches a maximum value  $Q_{o,max}$  at a distance of about 500 feet from the well. The ‘oil flow rate’ is the flow of **stock tank oil**, which is contained in both the gas and liquid phases in the reservoir. In this example, the maximum value occurs near to the outer edge of Region 2, but after the reservoir pressure falls below the dew point, Region 3 no longer exists and the maximum oil flow rate is found in the middle of Region 2.

In that part of Region 2 where the total oil flow rate is decreasing as the distance from the well reduces, some oil is condensed and is used to increase the size of Region 1. The amount of oil available is the difference between  $Q_{o,max}$  and the oil flow rate at the outer edge of Region 1.

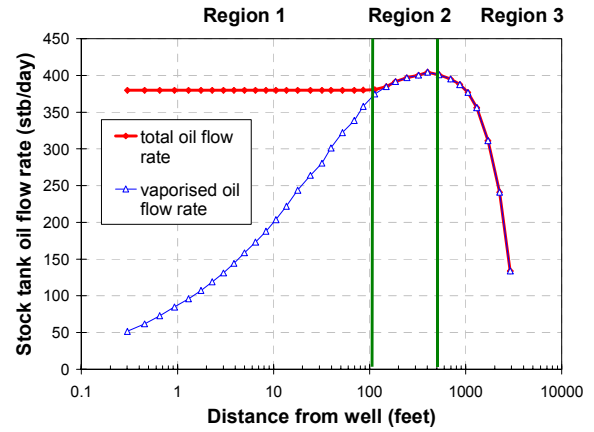


Fig. 3. Flow rate of stock tank oil to a vertical unfractured well.

We now consider how to calculate the expansion of Region 1 during the period  $\Delta t$  during which the average reservoir pressure declines from  $P_t$  to  $P_{(t+\Delta t)}$ .

The amount of oil (in stock tank barrels) which is condensed in Region 2 as gas flows towards the well is

$$X_o = [Q_{o,max} - Q_o(P_1)]\Delta t \quad (4)$$

In Region 2, the oil phase is immobile, but oil will be transported in the vapor phase. The flow rate of stock tank oil is

$$Q_o(P) = Q_g(P)r_{vsat}(P) \quad (5)$$

where  $Q_g(P)$  is the gas flow rate at a pressure  $P$ , which can be approximated by

$$Q_g(P) = Q_{gw} \left\{ 1 - \frac{PV(P)}{PV_{tot}} \right\} \quad (6)$$

where  $Q_{gw}$  is the gas flow rate at the well,  $PV(P)$  is the pore volume inside the pressure contour  $P$ , and  $PV_{tot}$  is the total pore volume of the well drainage area. Combining Eqs. 4 to 6 gives an expression for the amount of oil which is condensed in Region 2

$$X_o = \left\{ Q_{o,max} - Q_{gw}r_v(P_1) \left[ 1 - \frac{PV(P)}{PV_{tot}} \right] \right\} \Delta t \quad (7)$$

The amount of oil needed to expand Region 1 by a pore volume  $\Delta PV$  is

$$X_o = \Delta PV (S_{o,1} - S_{o,2}) \left[ \frac{1}{B_o(P_1)} - \frac{r_v(P_1)}{B_g(P_1)} \right] \quad (8)$$

$S_{o,1}$  is the oil saturation inside Region 1, estimated using Eq. 3.  $S_{o,2}$  is the oil saturation in Region 2, which is assumed to be the same as the saturation in a constant volume depletion experiment on the reservoir fluid (corrected to allow for the presence of connate water). Approximate values of the saturations are adequate to estimate the growth of Region 1. The term in square brackets in Eq. 8 is the derivative of the amount of stock tank oil with respect to the reservoir oil phase volume.

Combining Eqs. 7 and 8 gives a single equation with two unknowns - the increase in pore volume of Region 1, and the pressure at the edge of Region 1.

This can be solved if there is a way of calculating the pore volume inside a given pressure contour. This is done in terms of the ratio  $\alpha$ , defined as the fraction of the total drawdown which occurs inside the given pressure contour

$$\alpha = \frac{P - P_w}{P_{res} - P_w} \quad (9)$$

A table is set up giving pore volume as a function of  $\alpha$ . The values depend on the well type and the well and reservoir geometry, and the calculations are described in Appendix B.

A more accurate calculation can be obtained by replacing the pressure in Eq. 9 with the pseudopressure, to allow for the effect of condensate blockage on the pressure contours around the well. As the size of Region 1 is calculated in pressure steps decreasing from the initial reservoir pressure, the pseudopressure from the previous pressure step can be used in Eq. 9.

Guehria<sup>12</sup> also describes a way of calculating gas condensate well productivity, and estimates the flowing OGR by considering the flow within Region 1. The method in this work differs by calculating the volume of Region 1, which is the most significant parameter in determining the change in flowing OGR between the deep reservoir and near-well region.

**High-Velocity Effects.** The pseudopressure integral can be extended to model the two high-velocity effects that impact gas condensate well productivity – the increase in mobility at high capillary number and non-Darcy flow. The basic model is similar to that proposed in Ref. 13, where the gas phase velocity is estimated at each pressure point used in the numerical evaluation of the pseudopressure integral.

The capillary number  $N_c$  is then calculated using the equation

$$N_c = \frac{u\mu_g}{\phi(1 - S_{wmin})\sigma} \quad (10)$$

The gas-oil interfacial tension  $\sigma$  is obtained from a table versus pressure.

A number of empirical correlations have been proposed to model the change in relative permeability at high capillary number<sup>3,14,15</sup>. Any of these correlations can be used to adjust the calculation of  $k_{rg}$  and  $k_{ro}$  from the ratio  $k_{rg}/k_{ro}$ , to take account of the change in mobility with capillary number. However, it is simplest to use the correlation from Ref. 15, as it calculates  $k_{rg}$  as a function of  $k_{rg}/k_{ro}$  and capillary number.

The gas phase velocity is also used to estimate the impact of non-Darcy flow on the gas phase effective permeability – this correction is applied after  $k_{rg}$  has been calculated from  $k_{rg}/k_{ro}$  and  $N_c$ .

The calculation of gas phase velocity requires an estimate of the area of a given pressure contour, which depends on the well type and geometry. This is done by extending the table of pore volume versus fractional drawdown  $\alpha$  (defined in Eq. 9) to include the area of a pressure contour. The calculation of the area of pressure contours is discussed in Appendix B.

### Gas Condensate Well Productivity Spreadsheet

The material balance and well productivity models have been combined in an Excel spreadsheet for forecasting gas condensate reservoir performance. The spreadsheet can model three types of well geometry – a vertical unfractured well, a vertical fractured well, and a horizontal unfractured well.

The user must provide data for reservoir and well geometry, initial reservoir pressure, PVT properties, water and rock compressibility, relative permeability curves and parameters for models of high-velocity effects. The well can be controlled by rate, tubing head pressure or bottom hole pressure limits.

The spreadsheet calculates reservoir performance by stepping through the reservoir pressures in the black oil PVT table, in decreasing order from the initial reservoir pressure. At each pressure the spreadsheet estimates the size of Region 1 and the flowing OGR, then calculates the pseudopressure integral by numerical integration. The maximum gas production rate at that reservoir pressure is then calculated from the pseudopressure using Eq. 1. The maximum rates are used with a material balance calculation to calculate oil and gas production profiles as functions of time. An Excel macro is used to control these calculations.

### Comparison of Well Productivity Spreadsheet and Reservoir Simulation

The well productivity spreadsheet has been tested by comparison with results from fine-grid single-well compositional simulation for a number of different well types, gas condensate fluids and relative permeability models, and some typical results are presented in this section.

In all cases the Equation-of-State model from the reservoir simulator was used to calculate tables of PVT properties for the extended black oil model used in the spreadsheet. The oil viscosities were modified to reflect the lower values in the near-well region<sup>10</sup>, using a method described in Appendix C.

**Vertical Well.** The well productivity spreadsheet was used to estimate production profiles for a vertical well in a rich gas condensate reservoir. The reservoir model has a thickness of 60 feet and a permeability of 10 md. The outer radius of the well drainage area was 3500 feet.

The well was controlled with a maximum gas production rate of 15 MMscf/d, and a bottom hole pressure of 2000 psi. The fluid composition was taken from Ref. 16, with a dew point pressure of 6765 psi and an initial OGR of 165 stb/MMscf. Initial reservoir pressure was 8000 psi.

The well was completed throughout the reservoir thickness, so that the simulation model could use a 1-D radial grid, with 36 grid cells, equally spaced in log  $r$ . The smallest grid cell had a width of less than 1 inch.

Fig. 4 shows the production profiles calculated by the fine-grid simulation model and by the material balance spreadsheet, ignoring any high-velocity effects. Two sets of results are shown for the spreadsheet, using different approaches to calculate the pseudopressure integral – the CVDMB method and the new method to estimate the flowing OGR.

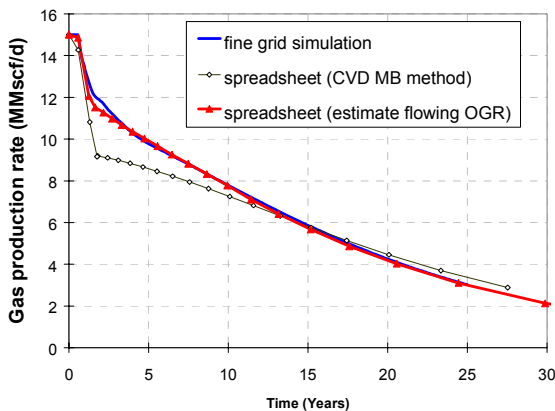


**Fig. 4.** Gas production profiles for vertical unfractured well, ignoring high-velocity effects.

The pseudopressure integral with the CVDMB method underestimates the well productivity, especially during the period after the well bottom hole pressure falls below the dew point. The new method, which estimates the flowing OGR by calculating the size of Region 1, gives much better agreement with the simulation results.

These calculations were repeated with relative permeabilities allowed to vary with capillary number, using the empirical model of Henderson *et al*<sup>1</sup>, and the results are shown in Fig. 5. These results demonstrate how the change in relative permeabilities with capillary number can lead to a significant improvement in the calculated well productivity. As before, the pseudopressure calculation is in good agreement with the simulation results, provided that the new method is used to estimate the flowing OGR.

In this example the inclusion of non-Darcy flow had only a small effect on the simulation results.

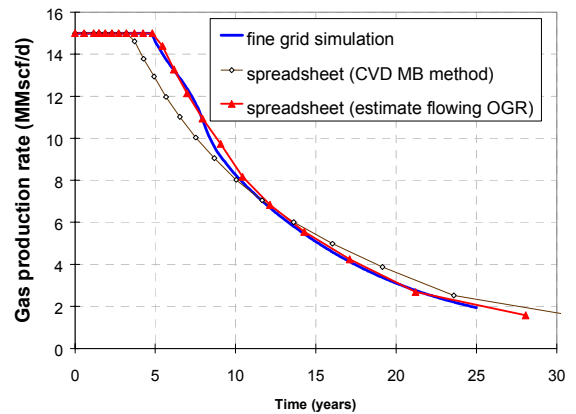


**Fig. 5.** Gas production profiles for vertical unfractured well, including the change in relative permeability with capillary number.

**Vertical Well with Hydraulic Fracture.** The second example is for a vertical well with a hydraulic fracture, in a lean gas condensate reservoir. The reservoir model has a thickness of 25 feet and a permeability of 1 md. The outer radius of the well drainage area was 2800 feet. The well was controlled by a maximum gas production rate of 6 MMscf/d and a bottom hole pressure of 1500 psi. The fluid had a dew point pressure of about 5000 psi and an initial OGR of 51 stb/MMscf. Initial reservoir pressure was 8000 psi.

The fracture was assumed to extend throughout the reservoir thickness. The simulation model used a 2-D grid in the x-y plane, with grid refinement near to the fracture. The smallest grid blocks, near to the tip of the fracture, measured 1 foot by 1 foot.

The fracture was represented explicitly in the simulation model by a plane of high-permeability grid cells. The width of these cells was increased to 1 foot, but the permeability was reduced so that the fracture conductivity (the product of permeability and fracture width) had the correct value. This approach has been used elsewhere for modeling hydraulic fractures in simulation models, in order to avoid the numerical stability problems associated with very small grid cells<sup>17,18</sup>.

A comparison between the results from the fine-grid compositional simulation model and the material balance spreadsheet is shown in Fig. 6. These results are for a fracture with a half-length of 100 feet and a conductivity of 15,000 md.feet. As in the previous example, the pseudopressure spreadsheet calculation gives reasonable agreement with the simulation results, provided that the new method is used to estimate the flowing OGR. The spreadsheet calculation underestimates well productivity slightly during the early production period, but the discrepancy is small compared with the other uncertainties in forecasting the performance of a fractured well.

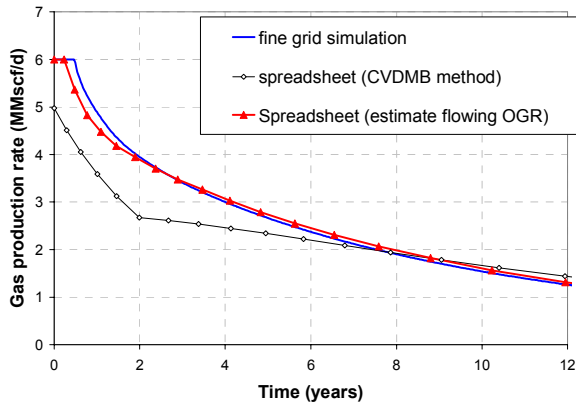


Fig. 6. Gas production profiles for fractured well, with fracture half-length = 100 ft.

For a fractured well in a low permeability reservoir, gas velocities around the well are much lower than for a radial well, so that high-velocity effects are usually not important. In this example, the inclusion of high-velocity effects made no significant difference to the results.

**Horizontal Well.** The third example is for a horizontal well in a low permeability, rich gas condensate reservoir. The well drainage area measured 5000 feet by 4000 feet, with a thickness of 100 feet.  $k_v / k_h$  was equal to 0.1.

The well was controlled by a maximum gas production rate of 20 MMscf/d and a bottom hole pressure of 2000 psi. The fluid had a dew point pressure of 6000 psi and an initial OGR of 207 stb/MMscf. Initial reservoir pressure was 9000 psi.

In the first calculation, horizontal permeability was 0.5 md and the well was 5000 feet long, and extended over the full length of the reservoir, so that a 2-D grid could be used in the reservoir simulation model.

The simulation grid used 27 grid cells in the horizontal direction and 15 in the vertical direction, and was refined around the well, with the well grid cell measuring 2 feet by 1 foot.

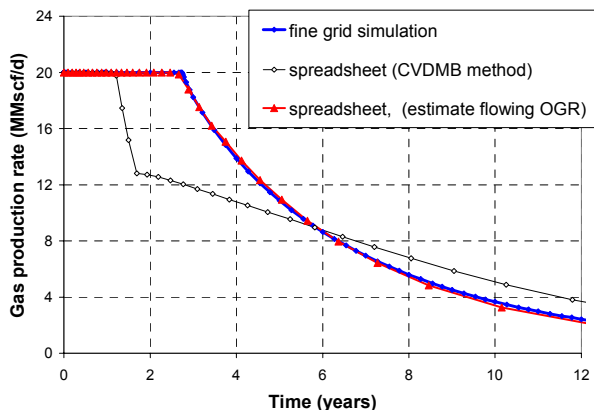


Fig. 7. Production profiles for horizontal well in rich gas condensate reservoir. Well length = 5000 feet,  $k_h=0.1$ md.

Fig. 7 compares the results for the spreadsheet and simulation models. As before, the spreadsheet is in good agreement with the simulation model, but only if the flowing OGR is estimated from the size of Region 1. The spreadsheet with the CVDMB method underestimates well productivity.

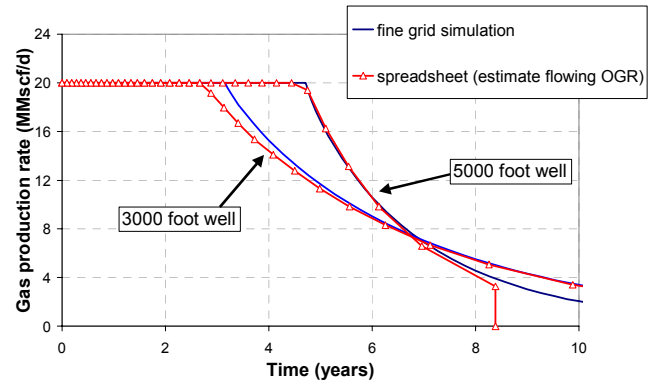


Fig. 8. Production profiles for horizontal well in rich gas condensate reservoir.

In the second set of calculations, horizontal permeability was 1 md and two different well lengths were examined – 3000 feet and 5000 feet. For the 3000 feet well a 3-D simulation grid was required, as the well did not extend over the full length of the reservoir. 20 grid cells were used in the direction parallel to the well, with the grid progressively refined around the tip of the well.

The results of these calculations are shown in Fig. 8. The spreadsheet calculation agrees quite well with the simulation results, although productivity is slightly underestimated for the shorter well.

## Summary and Conclusions

1. The performance of a gas condensate well can be forecast with a material balance model for reservoir depletion and a pseudopressure integral method for well inflow.
2. If the pseudopressure integral is to give accurate results, it is important to use the correct value of the flowing OGR in the near-well region. A new method has been developed for estimating the flowing OGR.
3. These techniques have been implemented in an Excel spreadsheet, which can be used to provide quick and accurate calculations of gas condensate well performance.
4. The spreadsheet has been tested by comparison with fine-grid numerical simulation for a number of cases, including hydraulically fractured and horizontal wells.

## Nomenclature

$B$	= formation volume factor
$C$	= units conversion factor
$h$	= net thickness
$h^*$	= net thickness of equivalent isotropic reservoir
$k$	= permeability
$k_r$	= relative permeability
$L$	= length of horizontal well
$m(P)$	= pseudopressure
$N_c$	= capillary number
$P$	= pressure
$P_{ref}$	= reference pressure for pseudopressure integral
$P_{res}$	= average reservoir pressure
$P_w$	= well flowing bottom hole pressure
$P_1$	= pressure at outer boundary of Region 1
$PV$	= pore volume
$Q_g$	= gas flow rate (Mscf/d)
$Q_o$	= stock tank oil flow rate (stb/d)
$r$	= distance from well
$r_e$	= external radius of well drainage area
$r_{skin}$	= radius of damaged zone
$r_v$	= oil-gas ratio
$r_{vF}$	= flowing oil-gas ratio in Region 1
$r_w$	= wellbore radius
$R_g$	= gas-oil ratio
$S$	= skin (Eqs. A-1 and A-2)
$S$	= saturation (other Eqs.)
$S_{wmin}$	= minimum water saturation
$u$	= Darcy velocity
$w$	= width of reservoir (perpendicular to horizontal well)
$X_o$	= amount of oil condensed in Region 1 (stb)
$\alpha$	= fractional drawdown to well (defined in Eq. 9)
$\beta$	= slope of pressure versus radius plot
$\phi$	= porosity
$\Phi$	= pressure potential
$\gamma$	= well completion-connection factor
$\mu$	= viscosity
$\theta$	= angle at well (see Fig A-2)
$\sigma$	= gas-oil interfacial tension

## Subscripts

$g$	= gas phase
$h$	= horizontal
$o$	= oil phase
$v$	= vertical

## Acknowledgements.

Financial support for this work was provided by BP Exploration Operating Co, Petroleum Development Oman, Texaco North Sea UK, and the UK Department of Trade and Industry.

## References

- Henderson, G.D. *et al.*: "Measurement and Correlation of Gas Condensate Relative Permeability by the Steady State Method," *SPEJ*, June 1996, p191-201.
- Seavareid, A., Whitson, C.H. and Fevang, O.: "An Engineering Approach to Measuring and Modeling Gas Condensate Relative Permeabilities," paper SCA-9930, presented at the Society of Core Analysts conference, Golden, Colorado, August 2-4 1999.
- Henderson, G.D. *et al.*: "The Relative Significance of Positive Coupling and Inertial Effects on Gas Condensate Relative Permeabilities at High Velocity," paper SPE 62933, presented at the SPE Annual Technical Conference and Exhibition, Dallas, Texas, October 1-4 2000.
- Mott, R., Cable, A. and Spearing, M.: "Measurements and Simulation of Inertial and High Capillary Number Flow Phenomena in Gas-Condensate Relative Permeability," paper SPE 62932, presented at the SPE Annual Technical Conference and Exhibition, Dallas, Texas, October 1-4 2000.
- Salino, P.A.: "Modeling Gas Condensate Reservoirs - Reconciling Laboratory and Welltest Data," in *Optimisation of Gas Condensate Fields*, IBC UK Conferences Ltd, London, January 1999.
- Skaar, R.G., Walpot, K.S. and van der Post, N.: "Matching Production Rates from the Saih Rawl and Barik Gas-Condensate Fields using a State-of-the-Art Single Well Reservoir Simulation Model," paper SPE 63163, presented at the SPE Annual Technical Conference and Exhibition, Dallas, Texas, October 1-4 2000.
- Cable, A.S., Mott, R.E. and Wickens, L.M.: "Field Model Predictions to Demonstrate the Value of Integrated Gas Condensate Near-Well SCAL Data," paper SCA-9930, presented at the International Symposium of the Society of Core Analysts, Monterrey, California, September 22-25, 2002.
- El-Banbi, A.H. *et al.*: "Producing Rich Gas-Condensate Reservoirs – Case History and Comparison between Compositional and Modified Black Oil Approaches," paper SPE 58955, presented at the SPE International Petroleum Conference and Exhibition, Villahermosa, Mexico, Feb 1-3, 2000.
- Fevang, O., Singh, K. and Whitson, C.H.: "Guidelines for Choosing Compositional and Black-Oil Models for Volatile Oil and Gas-Condensate Reservoirs," paper SPE 63087, presented at the SPE Annual Technical Conference and Exhibition, Dallas, Texas, October 1-4 2000.
- Fevang, O. and Whitson, C.H.: "Modeling Gas Condensate Well Deliverability," *SPE*, November 1996, p 221-230.

11. Mott, R.: "Calculating Well Deliverability in Gas Condensate Reservoirs," 10<sup>th</sup> European Symposium on Improved Oil Recovery, Brighton, UK, August 18-20 1999.
12. Guehria, F.M.: "Inflow Performance Relationships for Gas Condensates," paper SPE 63158, presented at the SPE Annual Technical Conference and Exhibition, Dallas, Texas, October 1-4 2000.
13. Whitson, C.H., Fevang, O., and Seavareid, A.: "Gas Condensate Relative Permeability for Well Calculations," paper SPE 63087, presented at the SPE Annual Technical Conference and Exhibition, Houston, Texas, October 3-6 1999.
14. Blom, S.M.P. and Hagoort, J.: "How to Include the Capillary Number in Gas Condensate Relative Permeability Functions," paper SPE 49268, presented at the SPE Annual Technical Conference and Exhibition, New Orleans, Louisiana, September 27-30 1998.
15. Whitson, C.H. and Fevang, O.: "Generalised Pseudopressure Well Treatment in Reservoir Simulation," IBC Technical Services conference on Optimisation of Gas Condensate Fields, Aberdeen, UK, June 1997.
16. Whitson, C.H. and Torp, S.B.: "Evaluating Constant Depletion Data", *JPT*, (March 1983) p 610.
17. Hegre, T.M.: "Hydraulically Fractured Horizontal Well Simulation", paper SPE 35506, presented at the European 3-D Reservoir Modeling Conference, Stavanger, Norway, April 1996.
18. Kroemer, E. *et al*: "Compositional Simulation of Well Performance for Fractured and Multiple Fractured Horizontal Wells in Stratified Gas Condensate Reservoirs", SPE 37995, presented at the SPE Reservoir Simulation Symposium, Dallas, Texas, June 1997.
19. Joshi, S.D.: *Horizontal Well Technology*, PennWell Books, 1991.
20. Babu, D.K. and Odeh, A.S.: "Productivity of a Horizontal Well", *SPEE*, (November 1989), p 417-421.
21. Prats, M.: "Effect of Vertical Fractures on Reservoir Behavior – Incompressible Fluid Case", *SPEJ* (June 1961), p 105-118.
22. Joshi, S.D.: "Augmentation of Well Productivity with Slant and Horizontal Wells", *JPT* (June 1988), p 729-739.

### Appendix A. Well Completion Connection Factors.

The well productivity spreadsheet allows for three types of well geometry – a vertical unfractured well, a vertical fractured well, and a horizontal unfractured well.

A vertical well is assumed to have a cylindrical drainage volume, with the well completed throughout the interval. For a vertical unfractured well

$$\gamma = \frac{2\pi Ckh}{\ln(r_e) - \ln(r_w) - 0.75 + S} \quad (\text{A-1})$$

$C$  is a constant for units conversion, which in field units equals 0.001127. This assumes  $Q_g$  has units of Mscf/d, and  $m(P)$  has units of psi.Mscf/(rb.cp).  $r_e$  is the external radius of the well drainage area.

For a fractured vertical well  $\gamma$  is calculated from Eq. A-1, but the wellbore radius is replaced by the 'equivalent wellbore radius', the radius of an unfractured well which would have the same productivity. The equivalent wellbore radius is calculated using the correlation presented by Joshi<sup>19</sup> in terms of the fracture half-length and dimensionless conductivity.

For a horizontal well, the model reservoir is assumed to have a 'shoe box' shape, and  $\gamma$  is calculated from the correlation of Babu and Odeh<sup>20</sup>.

### Appendix B. Pressure Distribution around a Well.

The calculation for the flowing OGR requires a method of estimating the pore volume inside a given pressure contour. In addition, the area of a pressure contour is needed to estimate the gas velocity at a given pressure. These data are obtained from tables of pore volume and area against the fractional pressure drawdown  $\alpha$  (defined by Eq. 9). These tables are calculated using some simplifying assumptions about the pressure distribution around a well, which are discussed here. These calculations assume single-phase flow and ignore changes in fluid properties with pressure.

**Vertical unfractured well.** In this case the pressure contours are cylinders. We assume that any mechanical skin is due to a zone around the well with a different permeability. If the radius of this zone is  $r_{skin}$ , the relationship between pressure and log(radius) is modeled by two straight lines, as shown in Figure A-1. The slopes of the lines are given by  $\beta_1$  in the outer zone and  $\beta_2$  in the inner zone, where

$$\beta_1 = \frac{P_{res} - P_w}{\ln r_e - \ln r_w + S} \quad (\text{A-2})$$

$$\beta_2 = \frac{P_{res} - P_w - \beta_1(\ln r_e - \ln r_{skin})}{\ln r_{skin} - \ln r_w} \quad (\text{A-3})$$

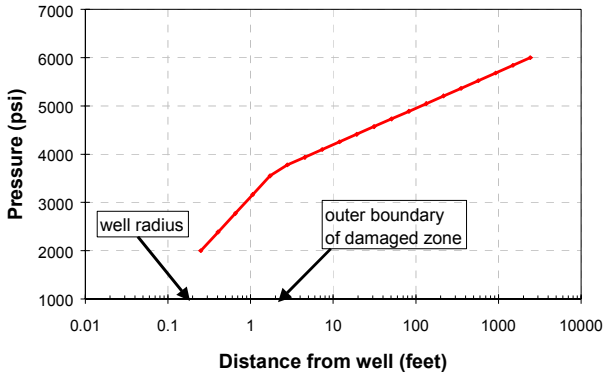


Fig A-1. Pressure distribution around a vertical unfractured well with skin from formation damage.

**Vertical fractured well.** Prats<sup>21</sup> gives a graphical plot of pressure potential contours around an infinite conductivity fractured well, up to a dimensionless distance ( $x/L$ , where  $L$  is the fracture half-length) of 2.5. The pressure contours are assumed to be ellipses. Outside of this region, the pressure is assumed to vary linearly with the log of the radius.

For each value of the potential, the major and minor axes of the ellipse (as dimensionless distances  $x/L$  and  $y/L$ ) are read from tables derived from Fig. 4 in Ref. 21. They can then be used to calculate the volume inside the pressure contour and the area of the pressure contour.

**Horizontal well.** The pressure contours round a horizontal well are estimated by considering a 2-D cross section in a vertical plane perpendicular to the well. The 2-D cross section is shown in Fig. A-2. Joshi<sup>22</sup> presents a steady-state solution for the pressure potential in this plane, for a well of length  $L$  where the reservoir width  $w$  is much greater than the thickness  $h$ . We have modified this to allow for a semi-steady-state solution, where the pressure gradient is zero at the outer reservoir boundary.

For an anisotropic system, when  $k_v$  is not equal to  $k_h$ , we can convert to the equivalent isotropic system by scaling the  $z$  axis. The reservoir thickness is now  $h^*$  where  $h^* = h\sqrt{k_h/k_v}$ .

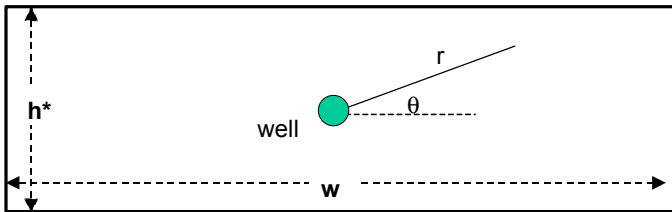


Fig A-2. Potential calculation for horizontal well.

The pressure potential is given by

$$\Phi(r, \theta) = \left( \frac{\pi \cos \theta}{h^*} \right) \left[ 1 - \frac{r \cos \theta}{w} \right] + \ln \left( \frac{\pi r}{h^*} \right) \quad (\text{A-4})$$

The potential varies with the log of radius near to the well, and linearly with radius far from the well. At the reservoir boundary  $r \cos \theta = w/2$ , and the pressure gradient is zero.

When  $2r < h^*$ , the cross section of the pressure contour is a circle. When  $2r > h^*$ , the contour is the intersection between a rectangle and a circle. When  $2r < h^*$ , the volume inside the pressure contour is

$$V = \sqrt{k_v/k_h} \pi r^2 L \quad (\text{A-5})$$

When  $2r > h^*$  it is

$$V = \sqrt{k_v/k_h} L \left\{ \frac{1}{2} r^2 \sin^{-1} \frac{h^*}{2r} + h^* \sqrt{r^2 - \left( \frac{h^*}{2} \right)^2} \right\} \quad (\text{A-6})$$

(The initial  $\sqrt{k_v/k_h}$  term is to convert the volumes back to the original reservoir geometry with thickness  $h$ ). The area of the pressure contour is given by

$$A = L \min \left[ 2\pi \sqrt{(1 + k_v/k_h)/2}, 2h \right] \quad (\text{A-7})$$

The potential is in arbitrary units, so a numerical integration is used to calculate the average potential in the reservoir, in order to be able to relate potential to pressure and hence to the fractional drawdown  $\alpha$ .

### Appendix C. Oil Viscosities in the Near-Well Region.

The extended black oil model assumes that fluid PVT properties are functions only of pressure. Tables of black oil PVT properties can be calculated by using an EoS model to simulate a constant volume depletion (CVD) test<sup>16</sup>. However, the oil composition in the near-well region is not necessarily the same as the composition in a CVD test at the same pressure, resulting in lower oil viscosities<sup>10</sup>.

In most gas condensate reservoirs, oil is immobile away from the well, so that oil viscosity is only relevant for flow near to the well (in Region 1). More accurate oil viscosities for the near-well region can be derived by using the EoS model to simulate a two-stage depletion process – a CVD down to pressure  $P_1$ , followed by a constant composition expansion of the gas phase at pressure  $P_1$ . This will give a set of tables of oil viscosity versus pressure, for different values of  $P_1$ . The lowest values from this set of tables are used for the oil viscosities in the black oil simulation.

In practice, these differences in oil viscosity may not be significant, especially as oil viscosities are often not measured for gas-condensate systems. However, the correct oil viscosities are important when comparing results calculated with black oil and compositional simulation models.